

# Nonlinear collision analysis of heavy trucks onto steel highway guard fences\*

Yoshito Itoh<sup>†</sup> and Chunlu Liu<sup>‡</sup>

Center for Integrated Research in Science and Engineering, Nagoya University, Nagoya 464-8603, Japan

Koichi Usami<sup>‡†</sup>

Department of Civil Engineering, Nagoya University, Nagoya 464-8603, Japan

**Abstract.** The design specifications of guard fences in Japan were reexamined and the revised specifications were implemented from April 1999. Because of the huge consumption in time and cost to test the performances of full-scale guard fences in the field, some assumptions are adopted while modifying the design specifications, and numerical analyses are necessary to confirm the impact performance and safety level of new types of steel highway guard fences. In this study, the finite element models are developed for the heavy trucks and steel highway guard fences to reenact their behaviors, and the solution approach is carried out using nonlinear dynamic analysis software of structures in three dimensions (LS-DYNA). The numerical simulation results are compared with the full-scale on-site testing results to verify the proposed analysis procedure. The collision process is simulated and it is also made possible to visualize the movement of the truck and the performances of guard fences. In addition, the energy shift of the truck kinetic energy to the truck and guard fence Internal energy, and the energy absorption of each guard fence component are studied for the development of a new design methodology of steel highway guard fences based on the energy absorption capacity.

**Key words:** dynamic analysis; energy absorption; finite element method; guard fence; heavy truck; non-linear analysis; vehicle collision impact.

---

## 1. Introduction

With the improvement of the road network and vehicle capacities, the heavy trucks have taken a more important role in the local and national freight transport. In Japan, the change of the allowable weight of trucks from 20 tf to 25 tf from November 1994 has increased the number of heavy trucks and the trucks with high gravity centers. Accordingly, from both the function and safety viewpoints, these changes challenge the conventional transportation infrastructures such as roads, bridges, and guard fences. For example, among the 2275 traffic facility accidents due to the impact between vehicles and static facilities in 1997 in Japan, 577 accidents happened with the guard fence according to the *Traffic Statistics* (1998). Fig. 1 shows the changes of traffic accidents and vehicle

---

<sup>†</sup> Professor  
<sup>‡</sup> Lecturer  
<sup>‡†</sup> Graduate Student

\*The earlier version of this paper appears in proceedings of EASEC-7, 27-29 August 1999, Kochi, Japan.

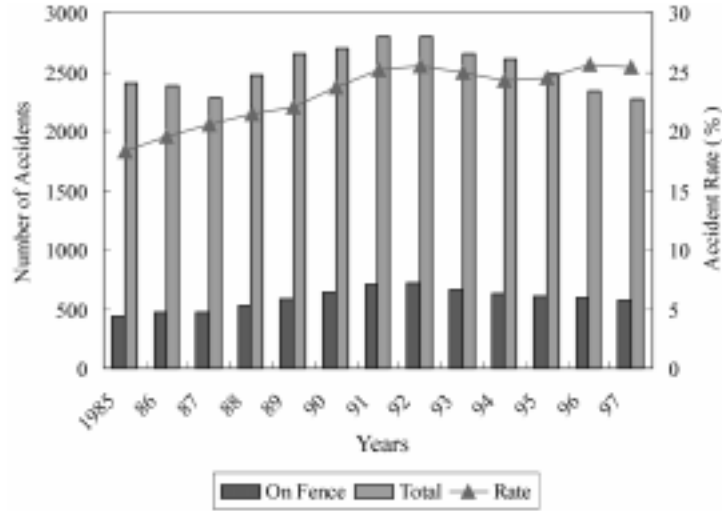


Fig. 1 Traffic accidents in Japan

impacts onto guard fences, and their ratios from 18.3% in 1985 to 25.4% in 1997 in Japan. Furthermore, the increases of the traffic speed, the large-scale and heavy trucks, the improvement of vehicular performances, and the high gravity centers of trucks also challenge the design and analysis of highway guard fences. Therefore, to take into consideration these changes into the design and construction of new highway guard fences, the design specifications of guard fences in Japan were reexamined and the revised specifications were implemented from April 1, 1999 to replace the former design guideline published in 1972 as shown in Fig. 2 (JRA 1999). However, because of the huge consumption in time and cost to test the performances of full-scale guard fences in the field, it is difficult in the field to measure the collision performances of the full-scale guard fences for various cases and some assumptions must be adopted while modifying the design specifications. Numerical analyses are necessary to confirm the impact performance and safety level of new types of steel highway guard fences for their design. Further, it is also very important to study the impact

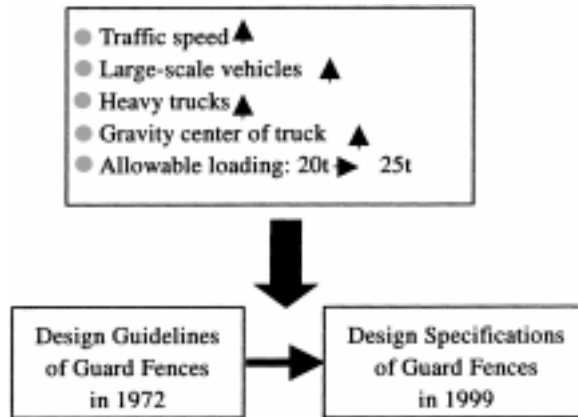


Fig. 2 Development of design specifications



Fig. 3 Existing guard fences

performance and safety level of the existing guard fences that were designed under the old guidelines and are taking effect in the field.

In the previous research in this field, several approaches have been carried out such as on the simulation of the impact load characteristics based on the experimental results of automotive vehicles (Miyamoto *et al.* 1991), and the impact response analysis for the shock softening type precast concrete guard fences (Kobayashi *et al.* 1994). Further study was also carried out on the impact simulation between vehicles and roadside safety hardware (Wekezer *et al.* 1993, Reid *et al.* 1996), a finite element computer simulation for the vehicle impact with a roadside crash cushion (Miller and Carney 1997), and a procedure for identifying the critical impact points for longitudinal barriers (Reid *et al.* 1998). In fact, there exist several types of guard fences as shown in Fig. 3. Both Figs. 3(a) and 3(b) are deflective guard fences. The concrete rigid guard fence as shown in Fig. 3(c) represents a typical type of rigid guard fences.

This research mainly focuses on the steel bridge guard fences as shown in Fig. 3(b). The rest of this paper is organized as follows. In the following section, a brief review is given on the development of design specifications of guard fences in Japan. By taking the advantages of both computer software and hardware, the collision impact process between the heavy trucks and the guard fences is simulated based on the presented numerical calculation models for both the heavy trucks and guard fences in section 3. The fourth section discusses the effects of the strain rates and mesh sizes on the displacement of the guard fence components by using a nonlinear, dynamic, three-dimensional finite-element code LS-DYNA (Hallquist 1999). In section 5, the analysis results are further compared with the full-scale experimental results using a real truck in order to demonstrate the approach presented in this research. In section 6, the energy shift of the truck kinetic energy to the truck and fence Internal energy, and the energy absorption of each guard fence component are studied for the development of a new design methodology of steel highway guard fences based on the energy absorption capacity. Finally, the seventh section concludes this study.

## 2. Development of design specifications of guard fences in Japan

The speed of road construction in Japan was rapidly increased from the first five-year highway construction plan started from 1954. Due to the increased traffic volume and traffic speed, the traffic congestion and traffic accidents increased year by year, and the highway guard fence became one indispensable structural component during the design, construction, or service and monitoring of the

Table 1 Changes of type S guard fence

	Type	Vehicle weight (tf)	Design speed (km/h)	Collision angle (degree)	Design impact energy (kJ)
Guideline in 1972	S	14	80	15	232
	SC		50		160
Specifications in 1999	SB	25	65	15	280
	SA		80		420
	SS		100		650

road infrastructure. To cope with the design and analysis demands of guard fences, the first version of design guideline of guard fences in Japan was implemented in 1965. It was revised twice in 1967 and 1972. The evolution of knowledge of roadside safety and performance evaluations was reflected in these guidelines. In recent years, several obvious changes have challenged civil engineers in the structural design and safety analysis of highway guard fences. These changes consist of the increases of the traffic speed, the large-scale vehicles and heavy trucks, the improvement of vehicular performances, and the height of the center of gravity of trucks. Therefore, to take into consideration these changes into the design and construction of new highway guard fences, the design specifications of guard fences in Japan were reexamined and the revised specifications were implemented from this financial year starting on April 1, 1999.

There were four types of guard fences used in the roadside in the previous design guideline, which were called Types A, B, C, and S of guard fences. In the new design specifications, the Type S is further classified as Types SA, SB, SC, and SS, which are appropriate for the increase of allowable loading from 14 tf in 1972 to 25 tf in 1999. Table 1 shows the changes of main criteria on Type S of guard fences from the previous design guideline in 1972 to the present design specifications in 1999. Specially, Type SS is one type of high strength guard fence in case that the vehicle weight is 25 tf and the design impact speed is 100 km/h. This type of guard fences is usually constructed for the highway bridge over-crossing super express railways. The performance of a guard fence is usually defined by its design impact energy, which is a quantitative criterion to reflect the strength of a guard fence from the energy point of view. The design impact energy can be defined as follows:

$$I_s = \frac{1}{2} \cdot m \cdot \left( \frac{V}{3.6} \cdot \sin \theta \right)^2 \quad (1)$$

where, the symbol  $I_s$  is the design impact energy;  $m$  is the quality of the design impact vehicle;  $V$  is the collision speed of the vehicle; and  $\theta$  is the impact angle. Table 2 shows the design impact energy of these seven types of guard fences used in the roadside. In the new design specifications in 1999, the construction site of the guard fence is classified into three types that are (1) the general site, (2) the potential large accident site, and (3) the site to be across or near the express railway. In the previous design guideline of guard fences in 1972, only types (1) and (3) are available. The proper site of each type of guard fences is shown in Table 3. The characters in the brackets represent the guard fence type in the previous design guideline.

In the design specifications of guard fences, the shape of the guard fence is not restricted. It can be decided by the designers according to the cost, road landscape, and others. However, the performances of a guard fence have to satisfy the following four requirements: (1) to prevent the

Table 2 Design impact energy of guard fences

Type	A	B	C	SS	SA	SB	SC
$I_s$ (kJ)	130	60	45	650	420	280	160

Table 3 Proper construction site of various types of guard fences

Types of roads	Design speed (km/h)	General site	Potential large accident site	Site across/near express railway
Expressway or exclusive motor-vehicle way	$\geq 80$	A (A)	SB	SS (S)
	$\leq 60$	A (B)	SC	SA (S)
General roads	$\geq 60$	B (B)	A	SB (S)
	$\leq 50$	C (C)	B	NA

Table 4 Basic criteria of impact accelerations

Type	Design speed (km/h)	Basic criteria of impact acceleration (g)
B, C	60	9-12
A	100	15-18
SC, SB, SA, SS	100	18-20

vehicle from breaking away from the road by controlling the strengthen and displacement performances; (2) to protect the passengers by restricting the impact acceleration effected onto the passengers from the vehicle; (3) to guide the movement of a vehicle after the impact by controlling the moving speed and angle of a vehicle; and (4) to prevent the components of guard fences from separating from the guard fences. Table 4 shows the fundamental criteria of the impact accelerations for various types of guard fences under the given impact speed. Similar to USA (TRB 1993), to the extent possible and practical, limiting values recommended for the respective evaluation criteria are also based on current technology and, when necessary, on the collective judgment of experts in roadside safety design in Japan. The adequacy of these or other criteria must ultimately be established by the agency responsible for the implementation of the safety device being evaluated. Inevitably, parts of the latest design and evaluation guidelines will be revised in the future with the emergence of new issues and the accumulation of human knowledge on roadside safety and performance evaluation.

### 3. Development of analysis models of steel highway guard fences and heavy trucks

#### 3.1 FEM Analytical model of guard fences

This research focuses on the collision impact of heavy trucks with a high speed onto the steel highway guard fences at the two sides of highways. The angle between the truck movement direction and the guard fence plane is an important parameter to determine the impact force and displacement in addition to the truck speed, the truck weight, the height of the gravity center of the

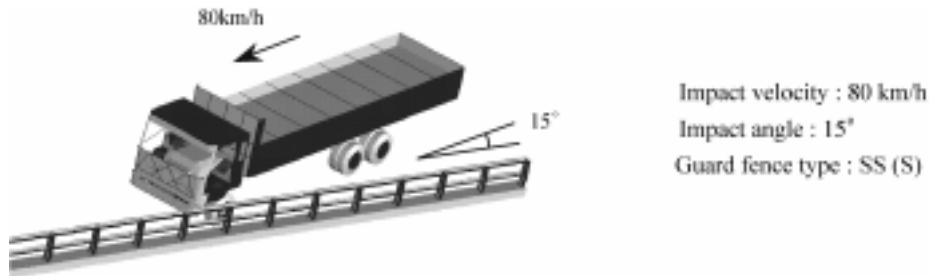


Fig. 4 Collision features

truck, the guard fence, the curb, and others. Fig. 4 shows the basic collision analysis components including a moving vehicle, the guard fence, the impact speed and the impact angle in this research.

In 1992, a structural model was presented for the steel bridge guard fences for the purpose of the full-scale experiment carried out in the Public Work Research Institute of Japan (1992). Then, a FEM analytical model based on the shell elements was formulated for the structural components of the steel bridge guard fences and the application procedure was presented in the previous research (Itoh *et al.* 1999). In the present research, a new hybrid FEM model based on both beam elements and shell elements instead of shell elements has been adopted in order to reduce the calculation time. As the beams and columns of fences that are far from the collision position are not of the local deformation, the beam elements are enough to keep the calculation accuracy for determining the global deformation. The numbers and locations of the spans of guard fences are shown in Fig. 5. Due to this revision, the FEM nodes and elements of the guard fences decrease from 10404 and 9621 to 6583 and 6152 respectively, and the calculation time of one case study is also reduced from about 70 hours to 55 hours. The computer platform is the workstation of Sun Ultra 450 whose clock is of three 300 MHz Ultra SPARC II (2MB Cache) (3CPU). Fig. 6a shows the cross section of a highway bridge guard fence. The fence column is made of the H-type steel whose web and flange are 158 mm wide and 6 mm thick, and 150 mm wide and 9 mm thick, respectively. Both the main

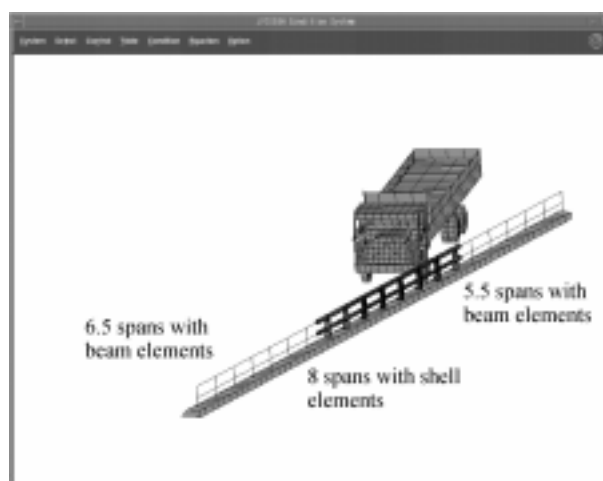


Fig. 5 Numbers and locations of spans with beam elements and shell elements

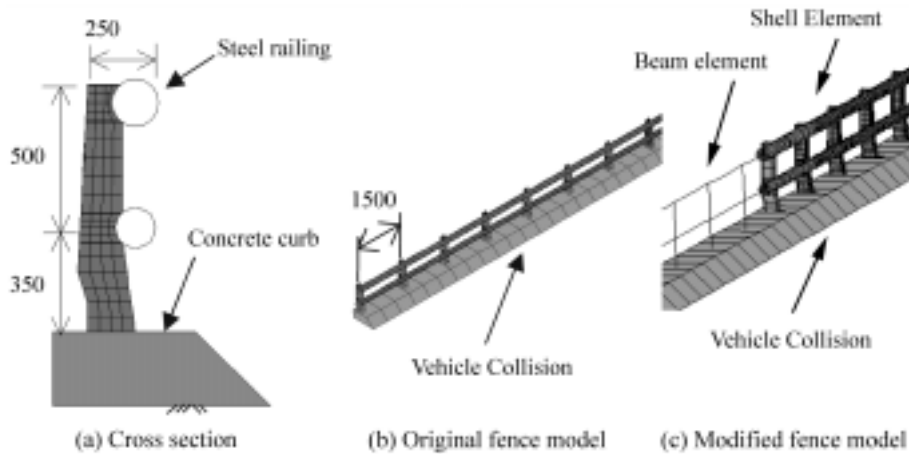


Fig. 6 Analysis model of guard fence (mm)

beam and sub-beam are of pipe sections. The pipe diameter and thickness of the main beam are 165 mm and 7 mm, respectively. The pipe diameter and thickness of the steel sub-beam are 140 mm and 4 mm, respectively. Figs. 6(b) and (c) represent the original and modified FEM models of the guard fences in three-dimensions. The span of the beams over two contiguous columns is 1500 mm.

The Young's modulus of steel is 206 GPa, and the Young's modulus of concrete is 24.4 GPa. The Poisson's ratios of steel and concrete are 0.3 and 1/6, respectively. The shear moduli of steel and concrete are 88 GPa and 10.5 GPa, respectively. The yield stress and initial strain hardening of steel are 235 MPa and 4.1 GPa, respectively. The strain hardening of steel starts from 0.0014. The concrete volume modulus is 12.2 GPa. The concrete compressive and tensile strengths are 23.5 MPa and 2.3 MPa, respectively. The steel is assumed to be an isotropic elasto-plastic material following the von Mises yielding condition. The strain hardening and strain velocity are taken into consideration the stress-strain relationship. The concrete constructed in the curb is assumed as a general elasto-plastic material. This means that the concrete is in the general elasto-plastic condition while the concrete in the compressive side reaches the yield point and only the cut-off stress is available once the tensile stress increases to the tensile strength. The boundary condition at the concrete curb is considered as a fixed end.

### 3.2 FEM Analytical model of trucks

In this research, the trucks with the weight of 25 tf are studied by modeling the truck frame, engine, driving room, cargo, tiers and so on. The structure of the 25 tf truck is similar to the 20 tf truck except the strengthened frame and the loading capacity of the vehicle vertical axles. As shown in Fig. 7, the truck is modeled according to the ladder-type truck frame with two side members of channel sections so that some facilities such as the fuel tanks and pipelines can be attached inside the side members. The thickness of the side member is 8 mm, and the yield stress is 295 MPa. The general elasto-plastic stress-strain relationship is adopted. The solid element with the same shape and volume is modeled for the engine and the transmission, and their weights are adjusted according to the practical vehicles. The tiers, wheels, and gears of a truck influence its behaviors during the collision impact significantly. The connection of the tier and the wheel is assumed to be

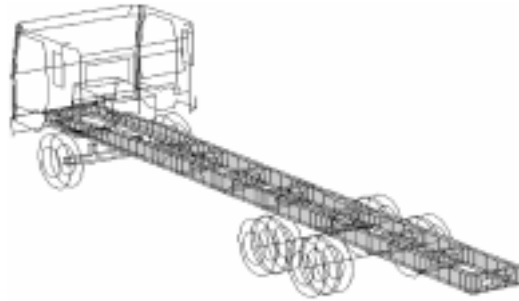


Fig. 7 Truck structural model

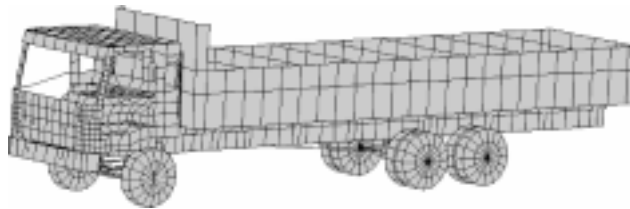


Fig. 8 Truck FEM model

a rotation joint so that the movement of the wheel can be simulated. A constant value of 0.45 is used for the friction coefficient between the tier and the road pavement. The driving room and other small portions are also modeled for the purpose of the numerical calculation.

Fig. 8 represents the presented FEM model of a heavy truck that will be used in the following of this paper. In this model, the numbers of nodes and elements are 3532 and 3904, respectively. The Young's modulus of steel is 206 GPa, while that of aluminum is 70 GPa. The Poisson's ratios of steel and aluminum are 0.30 and 0.34, respectively. The shear moduli of steel and aluminum are 88 and 26 GPa, respectively. In the case of guard fences, the steel is assumed to be an isotropic elasto-plastic material following the von Mises yielding condition, and the stress-strain relationship is perfectly elasto-plastic. The aluminum used for the cargo body is assumed in a multi-piece linear stress-strain relationship (Itoh *et al.* 1998).

#### 4. Nonlinear analysis of dynamic collision performances

##### 4.1 Effects of strain hardening and strain velocity

The study on dynamic collision performances is first carried out to check the effects of the strain hardening and strain velocity on the displacement of the guard fence components. It is assumed that the strain hardening starts from 0.0014 and the initial strain hardening modulus is 4.01 GPa (2% of the Young's Modulus). On the other hand, the yield stress usually increases with the increase of the strain velocity. In a previous study, materials tests for steel specimens under high-speed loadings were executed to explore the dynamic stress-strain relationships (Takahashi *et al.* 1991), and the recommended scaling relation of the yield stress as shown in Fig. 9 is used in this research to investigate the effects of the strain velocity.

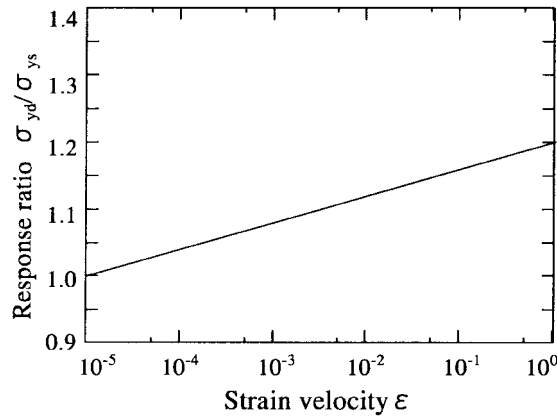


Fig. 9 Steel yield stress with strain velocity

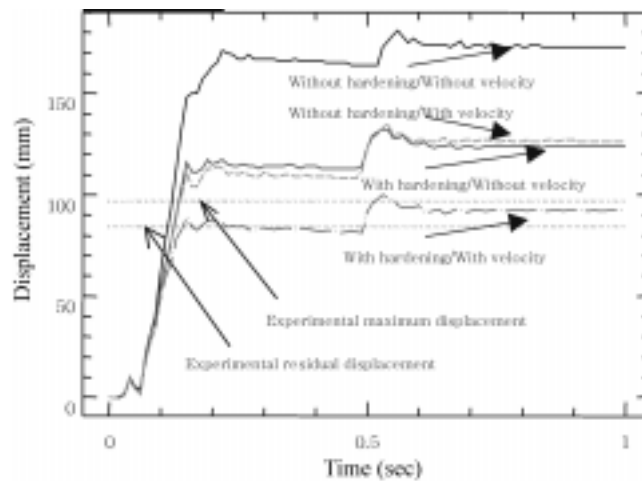


Fig. 10 Effects of strain hardening and strain velocity

Fig. 10 shows the displacement at the top of a column in the vertical direction to the guard fence plane with time in four combined cases by considering the strain hardening and strain velocity or not. This column coded as C10, whose position can be recognized from Fig. 11, is of the maximum displacement after the collision impact. In the calculation, the truck weight, collision speed and collision angle are 14 tf, 80 km/h and  $15^{\circ}$ , respectively. According to the displacement tracks as shown in Fig. 10, the effects of the strain hardening and strain velocity on the maximum response displacement and the residual displacement are very obvious. The displacements follow the similar tracks with time if one of the strain hardening and the strain velocity is considered and the other is eliminated. It should also be noticed that at about 0.5 second after the collision impact the displacement increases rapidly within a very short time at all cases. The experimental results are close to the results obtained by considering both the strain hardening and the strain velocity. Therefore, these two factors will be taken into account in the following part of this paper.

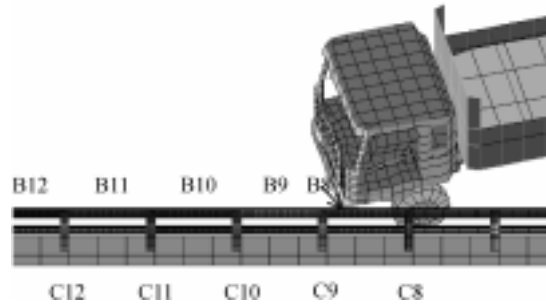


Fig. 11 Codes of columns and beams

#### 4.2 Effects of mesh sizes

Further study is carried out to determine the appropriate mesh sizes by following the tracks of the displacement of the bridge guard fence with time. The calculation results are compared with the experimental values by adjusting the mesh sizes of the column web, the column flange, and the horizontal beam pipe. Three cases, 1-2-8 model, 4-4-16 model and 8-8-32 model, are studied. The three numbers of each model represent the mesh numbers of the column web, column flange and beam pipe, respectively. The total numbers of FEM nodes of these three models are 5739, 10404, and 28125, respectively. Their total element numbers are 5158, 9574, and 27045, respectively. The calculation results are shown in Fig. 12 as well as the detected values from the actual experiment for the case when the truck weight, collision speed and collision angle are 14 tf, 80 km/h and  $15^\circ$ , respectively. Fig. 12 shows the displacement of only the column C10 at its top in the vertical direction to the guard fence plane. According to the displacement curves in Fig. 12, the residual response displacements in cases of 4-4-16 model and 8-8-32 model are very large at 0.5 second after the collision impact (about 40%). The tracks in these two cases are almost same within the first 0.5 second. The final displacement is about 10% less than the maximum value in all cases. Compared to the maximum and residual displacements from the experiment, the 4-4-16 model

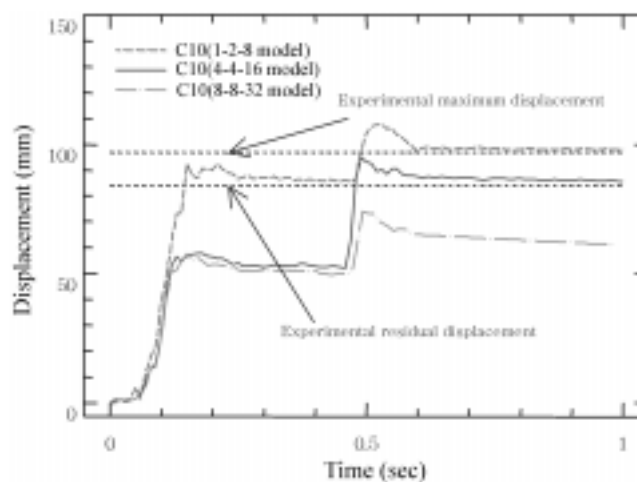


Fig. 12 Effects of mesh sizes

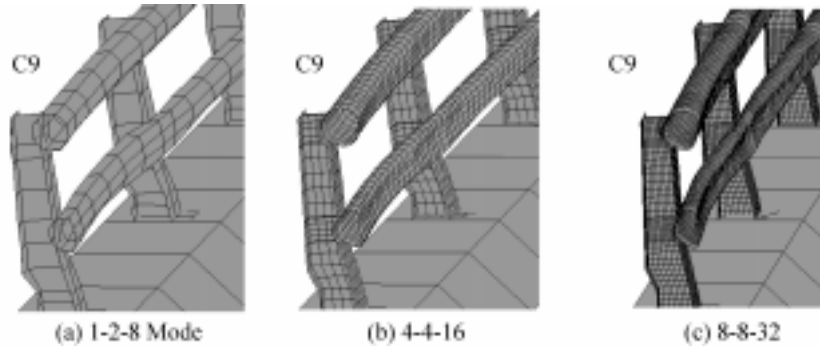


Fig. 13 Displacement of guard fences under three modes

contributes very good agreements. Therefore, this model will be adopted in the following analysis. Figs. 13(a), 13(b) and 13(c) show the visible displacement of the columns and beams of the guard fences in three different modes 1-2-8, 4-4-16 and 8-8-32, respectively.

## 5. Comparative studies with on-site testing

### 5.1 Movement track of a collision truck

For demonstrating the above-presented models, four numerical examples, FB14-80-15, FB25-65-15, FB25-80-15, and FB25-100-15 cases, are formulated and studied in this research. The three components in the type name of each case represent the type and weight of vehicles, the impact speed in kilometer per hour and the impact angle degree. Because the experimental data are available for the case FB14-080-15, the calculated results could be compared with the experimental results. Fig. 14 shows the moving track of a truck. The front of the truck first touches the guard fence and the front wheel runs onto the curb very soon and impacts the guard fence. Then, the truck frame inclines, the direction of movement is changed suddenly, and the rear wheel runs onto the curb. Finally, the rear wheel of the truck touches the guard fence and the sloped angle of the back truck frame increases so that the truck frame shifts the moving direction and leave the bridge guard fence. Fig. 15 shows the performances of both the truck and guard fences at several collision conditions in detail, which are 0, 0.2, 0.4, 0.6, 0.8 and 1.0 seconds. The graphs from the previous experiment carried out by the Public Works Research Institute in Japan and the simulation in the present research are compared.

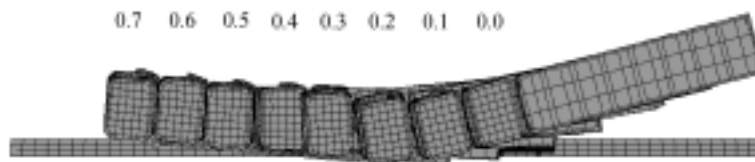


Fig. 14 Movement of a truck at various moments after the collision impact (second)

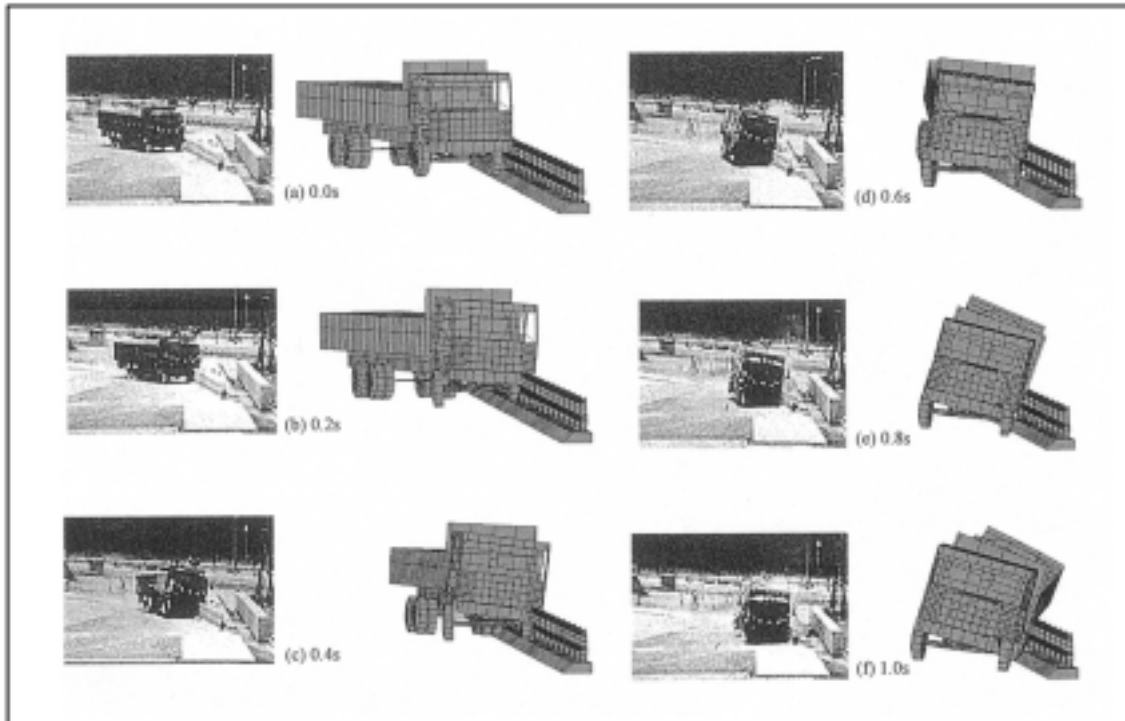


Fig. 15 Impact performance of a truck and the guard fence (Left: Experiment, Right: Simulation)

### 5.2 Displacement response of guard fence components

Fig. 16 compares the calculated results using the original model and the modified model in the research with experimental results carried out by the Public Works Research Institute in Japan. The impact performance of the guard fence after 0.7 second of the vehicle collision is shown in Fig. 16(a). Figs. 16(b), 16(c), and 16(d) represent the results of displacement responses using both the original and modified model for the columns at the top, the main beams and the sub beams, respectively. The results using the modified model are very similar with the results obtained from the original model for all the three piers as shown in Fig. 16(b). The results are also very similar in the cases of main beams and sub beams except the main beam B9 and sub beam B10 as shown in Figs. 16(c) and 16(d), respectively. However, two thirds of the calculation time is reduced. The experimental maximum and residual displacements are also shown in the figures for the purpose of comparison. As shown in Fig. 16(b), it is very obvious that the maximum and residual response displacements of the column C10 are very close to the practical vehicle experiment values 97 mm and 84 mm, respectively. In the cases of main beams and sub beams, the calculation value of the main beam B10 at the central section is about 30% higher than the detected value of 76 mm from the practical experiment. However, the calculated displacement value of the sub-beam B9 at the central section is about 20% less than the experimental value of 130 mm.

Using the FEM model of the bridge guard fences, the horizontal dynamic response force of column C9 in the vertical direction to the guard fence plane is calculated and compared with the practical experimental results as shown in Fig. 17. It is obvious that the calculated values and the

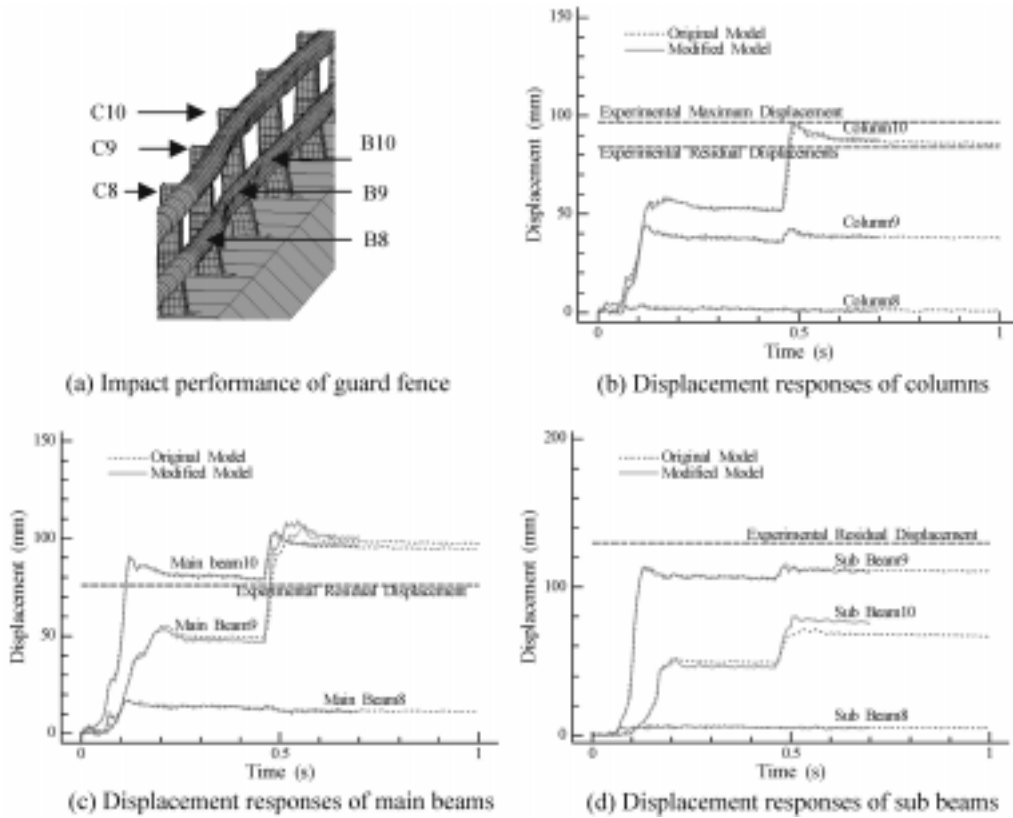


Fig. 16 Comparison of calculated results using original and modified models for FB14-80-15

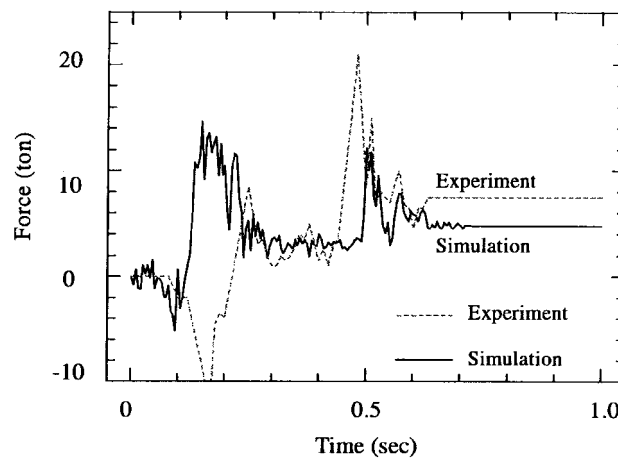


Fig. 17 Comparison of horizontal forces onto Column C9

experimental results are rather consistent within the first 0.1 second and after 0.2 second. However, the differences are quite large from 0.1 second to 0.2 second. This may result from the fact that the strain gauge is used to detect the shearing strain while the experimental horizontal force is

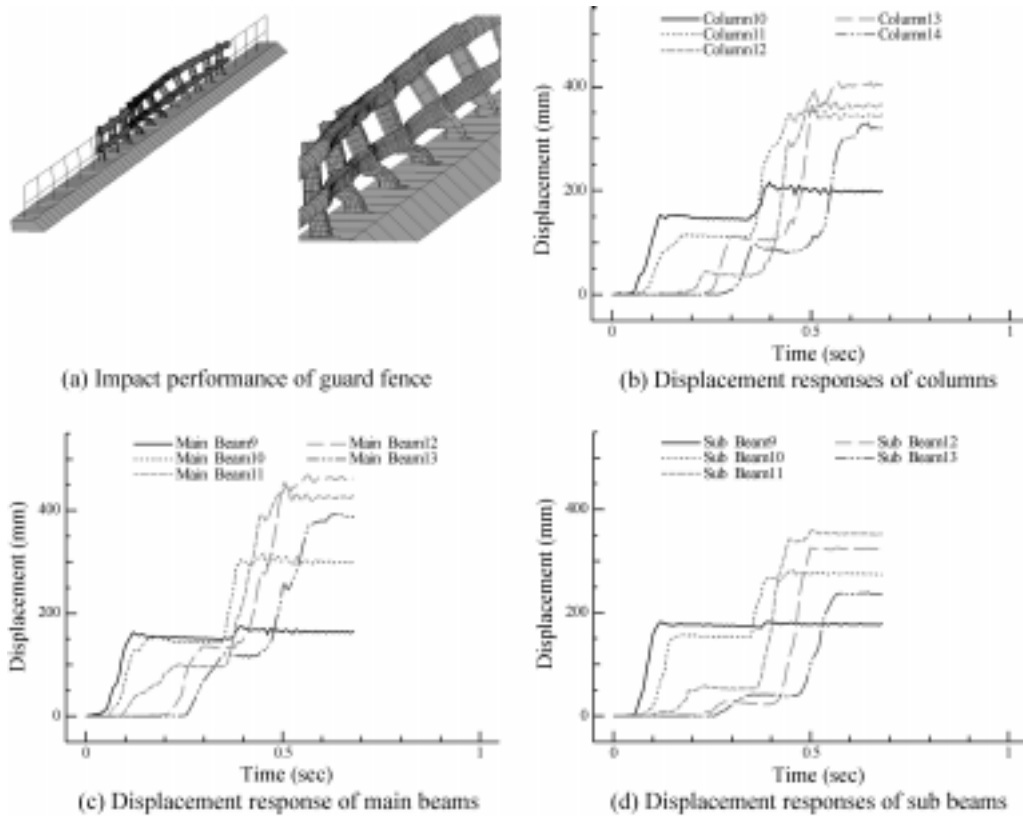


Fig. 18 Displacement responses of guard fences for FB25-100-15

determined, and the relationship between the load and the shearing force was modeled according to the static loading experimental results. After 0.6 second in both the experiment and the simulation, the forces are stable. This may represent that the dynamic impact response between the trucks and the guard fences last about 0.6 second.

## 6. Development of design methodology based on energy shift and absorption

Further study is carried out using other numerical examples by changing the weight and impact speed of vehicles. Fig. 18 shows the calculated results in the case of FB25-100-15 using the modified model. The impact performances of the guard fence after 0.1 and 0.5 seconds of the vehicle collision are shown in Fig. 18(a). Figs. 18(b), 18(c), and 18(d) represent the results of the displacement responses for the columns at the top, the main beams and the sub beams, respectively. The maximum residual displacements of columns, main beams and sub beams are 402 mm for Column C13, 470 mm for Main Beam B12, and 370 mm for Sub-beam B11, respectively. It can be noticed that these residual displacements are only a little bit less than the maximum displacements.

### 6.1 Energy absorption of bridge guard fence

The detail of energy absorption among the guard fence components with time is shown in Fig.

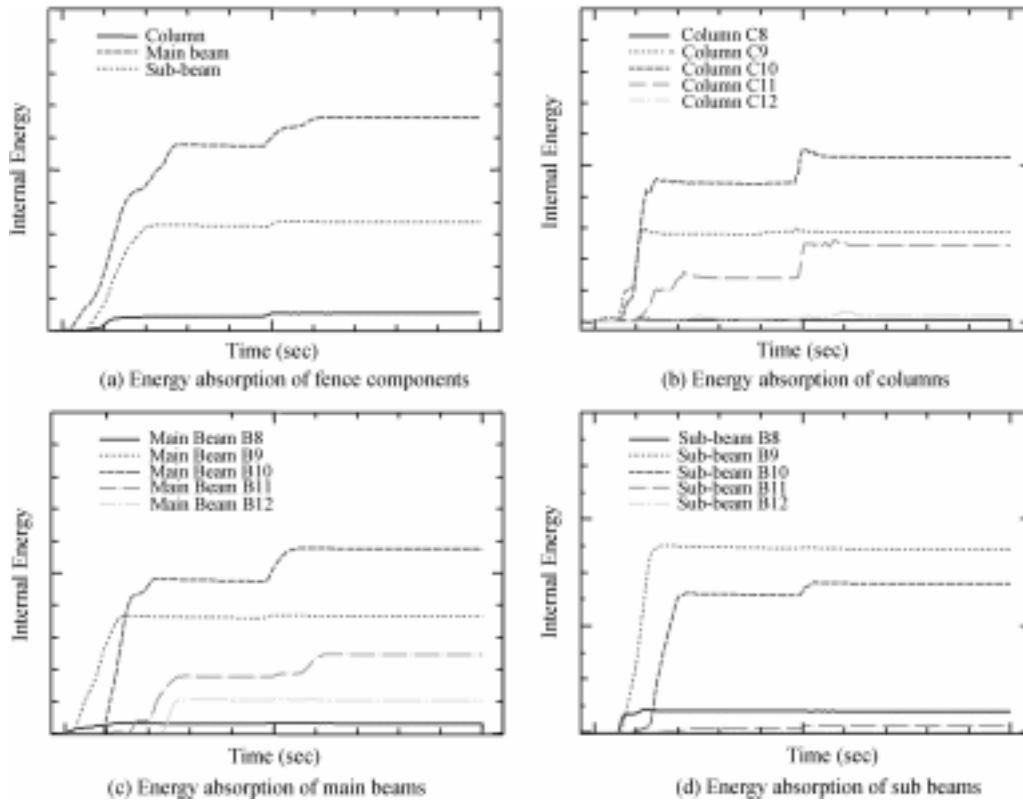


Fig. 19 Energy absorption of guard fence components

19(a). About 65%, 30%, and 5% of the impact energy are absorbed by the main beam, the sub-beam, and the fence column, respectively. This percentage distribution is related to the assumption that the truck collision impact starts from the main beam. Figs. 19(b), 19(c) and 19(d) show the energy absorption of several specific components of the columns, beams, and sub beams, respectively.

In Fig. 19(b), it can be seen that the column C10 absorbs more energy than other columns. About 50% of energy is absorbed by this column although C9 and C8 are the two nearest columns to the collision impact point as pointed out above in Fig. 12. At about 0.5 second after the collision impact, the energy consumption of both C10 and C11 increases suddenly within a short time. In the case of the main beam as shown in Fig. 19(c), the beam B10 absorbs about 50% of the energy. However, as shown in Fig. 19(d), the sub-beam B9 absorbs more than 50% of the energy absorbed by all sub-beams. It should be noticed that the energy absorption is consistent with the displacement curves as shown in Figs. 18(b), 18(c) and (d). For example, in both the displacement and the energy absorption, C10, B10 and B9 take the most important effects in columns, main beams, and sub-beams, respectively. Further, the order of columns C10, C11, C9, C12 and C8 according to the decrease of displacements is similar with the order C10, C9, C11, C12, and C8 in absorbing the internal energy. The main beam and the sub-beams have the similar characters of orders. This means that a column or beam that has a relatively large displacement may absorb relatively more energy than other columns or beams.

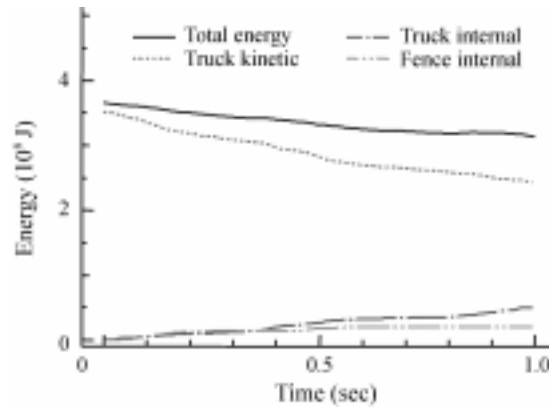


Fig. 20 Energy shift of truck kinetic to truck and fence internal

In addition, the energy shift of the truck kinetic to the truck and fence internal after the collision impact are studied and the results are shown in Fig. 20 for the case BF14-80-15. The truck internal is obviously larger than the fence internal after 0.4 second of the collision impact. The total energy including the truck kinetic, the truck internal and the fence internal continue to decrease until one second after the collision.

## 6.2 Analyses on calculation results

Table 5 shows the moving speed of a truck after 0.7 second of the impact collision, and the decreased percentages of speeds in both the movement direction and the vertical direction to the

Table 5 Moving speed of a truck after the impact collision

Cases	Impact speed (km/h)	Moving speed (0.7s) (km/h)	Decreased speed in movement direction (%)	Decreased speed in the vertical direction to guard fences (%)
FB14-080-15	80	70.3	10	83
FB25-065-15	65	54.1	14	79
FB25-080-15	80	70.5	10	74
FB25-100-15	100	86.7	10	73

Table 6 Energy absorption among vehicle and guard fences

Cases	Design impact energy (kJ)	Energy absorption (kJ)				Vehicle	Total energy absorption (kJ)
		Guard fence					
		Column	Main beam	Sub beam	Total		
FB14-80-15	232	18	101	85	204	324	880
FB25-65-15	273	5	100	80	185	672	1010
FB25-80-15	414	64	200	234	498	770	1530
FB25-100-15	647	220	360	450	1030	1080	2450

Table 7 Identified components with more energy absorption

Cases	Design impact energy (kJ)	Component and energy absorption (kJ)					
		Column		Main beam		Sub beam	
FB14-080-15	232	10	9	10	34	10	41
FB25-065-15	273	9	2.4	12	30	9	27
FB25-080-15	414	11	21	11	48	10	83
FB25-100-15	647	13	45	11	68	10	85

guard fence. It can be found that the decreased percentages of speeds in these two directions are about 10% and 80%, respectively. The impact energy of a vehicle due to its speed and weight will be distributed among the vehicle, column, main beam, and sub beam because a part of the movement energy is absorbed by the components of a guard fence. The detail of energy absorption among the vehicle and guard fence components in several cases is shown in Table 6. With the increase of the moving speeds of vehicles, a higher percentage of movement energy will be absorbed by the guard fence and a less percentage of the movement energy will be absorbed by the vehicles. In three cases of vehicles of 25 tf, more than 80 percentage of the movement energy is absorbed by both the vehicle or guard fence. However, this percentage is only 60% for a vehicle of 14 tons. Further, more energy is absorbed by the sub beams in the case of impact collision of a heavy truck or a fast truck.

It is also noticed that the distributions of energy absorption among various columns, main beams and sub beams change with the weight and speed of vehicles. Table 7 shows the components that absorb the most energy. Actually, the energy absorption is consistent with the displacement curves. For example, in both the displacement and the energy absorption, column C10, beam B10 and beam B9 take the most important effects in columns, main beams, and sub-beams, respectively. This means that a column or beam that has a relatively larger displacement may absorb more energy than other columns or beams. Further research effort is needed to develop the design methodology of steel bridge guard fences to involve the energy absorption capacity in future.

## 7. Conclusions

In this paper, the numerical analysis models are prepared for simulating the behaviors of both trucks and bridge steel guard fences due to the collision impact. The usefulness of these models is demonstrated via numerical examples. The following conclusions can be stated:

- (1) From the comparative studies of on-site experimental and numerical simulation results, it was made clear that both the strain hardening and strain velocity should be considered, and the mesh sizes also affect the accuracy of calculation results.
- (2) It is possible to simulate the collision process and to visualize the movement of the truck and the performances of bridge guard fences due to the collision impact of heavy trucks based on the newly developed FEM models for trucks and guard fences.
- (3) A high percentage of the collision impact energy is absorbed by the main beam of the guard fence, and the displacement of the main beam is also relatively large. The collapse of the main fence beam can effectively absorb the impact energy from the collision impact of a heavy truck.

## Acknowledgements

The partial financial support of the Ministry of Education, Science, Sports and Culture in Japan as the Foundation of Science Research (No. 11555124) is gratefully acknowledged.

## References

- Hallquist J. (1999), *LS-DYNA User's Manual (Version 950)*, Livermore Software Technology Corporation, The Japan Research Institute LTD.
- Itoh, Y., Mori, M., and Liu, C. (1999), "Numerical analysis on high capacity steel guard fences subjected to vehicle collision impact", *The Fourth Int. Conf. on Steel and Aluminium Structures*, Espoo, Finland, June, 53-60.
- Itoh, Y., Ohno, T., and Mori, M. (1998), "Numerical analysis on behavior of steel columns subjected to vehicle collision impact", *J. Struct. Eng.*, JSCE, 40A, 1531-1542 (in Japanese).
- JRA (1999), "Design specifications of guard fences", Japan Road Association, Tokyo (in Japanese).
- Kobayashi, K., Okuda, M., Ishikawa, N., and Hiruma, Y. (1994), "Impact response analysis for the model test of the shock softening type precast concrete guardfence", *J. Struct. Eng.*, JSCE, 44A, 1531-1542 (in Japanese).
- Miller, P., and Carney, J. (1997), "Computer simulations of roadside crash cushion impacts", *J. Transp. Eng.*, ASCE, 123(5), 370-376.
- Miyamoto, A., King, M., and Masui, H. (1991), "Numerical modeling of impact load characteristics acting on structures", *J. Struct. Eng.*, JSCE, 37A, 1531-1542 (in Japanese).
- Reid, J., Sicking, D., and Bligh, R. (1998), "Critical impact point for longitudinal barriers", *J. Transp. Eng.*, ASCE, 124(1), 65-72.
- Reid, J., Sicking, D., and Paulsen, G. (1996), "Design and analysis of approach terminal sections using simulation", *J. Transp. Eng.*, ASCE, 122(5), 399-405.
- Takahashi, Y., Ohno, T., Ohta, T., and Hino, S. (1991), "Strain-rate effects on elasto-plastic behaviors of reinforced concrete beams under impact loadings", *J. Struct. Eng.*, JSCE, 37A, 1567-1580 (in Japanese).
- Traffic Statistics* (1998), Institute for Traffic Accident Research and Data Analysis, Tokyo (in Japanese).
- TRB (1993), "Recommended procedures for the safety performance evaluation of highway features", NCHRP Report 350, Transp. Research Board, Washington.
- Wekezer, J., Oskard, M., Logan, R., and Zywickz, E. (1993), "Vehicle impact simulation", *J. Transp. Eng.*, ASCE, 119(4), 598-617.
- WRI (1992), "A study on the steel guard fences", Research Report No. 74, Public Works Research Institute, Tsukuba (in Japanese).